Available online at www.sciencedirect.com
SCIENCE DIRECT®
Journal of Power Sources 135 (2004) 88–94
JOURNAL OF POWER SOURCES
www.elsevier.com/locate/jpowsour

Neural networks-based control of active and reactive power of a stand-alone PEM fuel cell power plant

M.Y. El-Sharkh, A. Rahman*, M.S. Alam

Department of Electrical and Computer Engineering, University of South Alabama, 307 Univ. Blvd. N, Mobile, AL 36688-0002, USA

Received 16 February 2004; accepted 11 March 2004

Available online 19 June 2004

Abstract

This paper presents a neural networks (NN)-based active and reactive power controller of a stand-alone proton exchange membrane (PEM) fuel cell power plant (FCPP). The controller modifies the inverter modulation index and the phase angle of the ac output voltage to control the active and reactive power output from an FCPP to match the terminal load. The control actions are based on feedback signals from the terminal load, output voltage and hydrogen input. The validity of the controller is verified when the FCPP model is used in conjunction with the NN controller to predict the response of the power plant to: (a) computer-simulated step changes in the load active and reactive power demand, and (b) actual active and reactive load demand of a single family residence. The response curves indicate the load following characteristics of the model and the predicted changes in the analytical parameters highlighted by the analysis.
© 2004 Elsevier B.V. All rights reserved.

Keywords: Fuel cell; PEM fuel cell; Active and reactive power control; Fuel cell model; Neural networks

1. Introduction

The fuel cell, as a renewable energy source, is considered one of the most promising sources of electric power. Fuel cells are not only characterized by higher efficiency than conventional power plants, but they are also environmentally clean, have extremely low emission of oxides of nitrogen and sulfur, and have very low noise.

The main components of a proton exchange membrane (PEM) fuel cell system include the fuel processing unit or the reformer, the fuel cell stack and the power conditioning unit. In general, hydrogen fuel is produced by processing some hydrocarbon fuel such as propane, natural gas, or methanol in the reformer. During fuel processing, carbon monoxide is produced. Reduction of carbon monoxide to acceptable levels is achieved by the water-gas shift reaction.

The output from the fuel cell is dc power. When a fuel cell power plant (FCPP) provides power to a residential load, or to the electrical grid, a power conditioning unit is needed.

The power conditioning unit is simply a dc/dc converter used to raise the dc output voltage, which is generally the dc bus voltage, followed by a single-phase or three-phase dc/ac inverter. In grid parallel operation mode a transformer is needed because of the voltage difference between the fuel cell power plant output and the grid. Due to low working temperature (80–100 °C) and fast start up, PEM fuel cells are best suited for residential and vehicular applications. The reasons behind selecting the PEM FCPPs in this paper are: (a) fuel cell user's group publications indicate that for small residential application, where major heating appliances are natural gas operated, a 5 kW unit is adequate; (b) a 5 kW commercial PEM FCPP is currently operational in the authors' lab.

Many models have been proposed to simulate fuel cells in the literature. The basis of a model can be fluid dynamics, electrochemical reaction, heat transfer and thermal [1–10]. To study the transient response of a grid-independent PEM fuel cell power plant, this paper employs an electrochemical model for a 5 kW fuel cell, which incorporates an external reformer to generate hydrogen from methane.

To enable the FCPP to conform to the load changes, it is essential to control the active and reactive power output of the power plant. An active and reactive power control scheme has been developed in Ref. [11]. The control scheme is based on controlling the ac output voltage phase angle to control the power flow from FCPP to the connected load. The reactive power is controlled through controlling the inverter modulation index. This paper uses the same controlling

* Corresponding author. Tel.: +1-251-460-6117; fax: +1-251-460-6028.
E-mail address: arahman@usouthal.edu (A. Rahman).

0378-7753/$ – see front matter © 2004 Elsevier B.V. All rights reserved.
doi:10.1016/j.jpowsour.2004.03.071

scheme to develop a neural network (NN)-based controller to control the active and reactive power output of the FCPP.

The paper is organized as follows: Section 2 introduces a model for a fuel cell system. Section 3 presents the NN design and training process. Load following test results of this model are presented in Section 4. Section 5 presents the conclusions.

2. Fuel cell system model

2.1. Fuel cell model

In Ref. [6], Padulles et al. introduced a model for the SOFC. The model has been modified to simulate a PEM fuel cell [7]. This model is based on simulating the relationship between output voltage and partial pressures of hydrogen, oxygen, and water. A detailed model of the PEM fuel cell is shown in Fig. 1. The model parameters are as follows:

B, C	constants to simulate the activation overvoltage in PEM FC (A^{-1}) and (V) [7,10]
E_0	Standard no load voltage (V)
F	Faraday's constant (C/kmol)
I	stack current (A)
K_r	modeling constant (kmol/s A)
K_{H_2}	hydrogen valve molar constant (kmol/atm s)
K_{H_2O}	water valve molar constant (kmol/atm s)
K_{O_2}	oxygen valve molar constant (kmol/atm s)
N_0	number of series fuel cells in the stack
p_{H_2}	hydrogen partial pressure (atm)
p_{H_2O}	water partial pressure (atm)
p_{O_2}	oxygen partial pressure (atm)
q_{H_2}	input molar flow of hydrogen (kmol/s)
q_{O_2}	input molar flow of oxygen (kmol/s)
R	universal gas constant (l atm/kmol K)
R^{int}	stack internal resistance (Ω)
T	absolute temperature (K)
τ_{H_2}	hydrogen time constant (s)
τ_{H_2O}	water time constant (s)
τ_{O_2}	oxygen time constant (s)

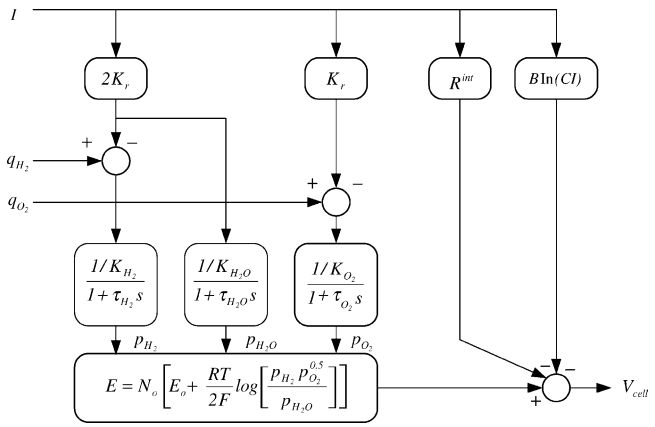

Fig. 1. PEM fuel cell model.

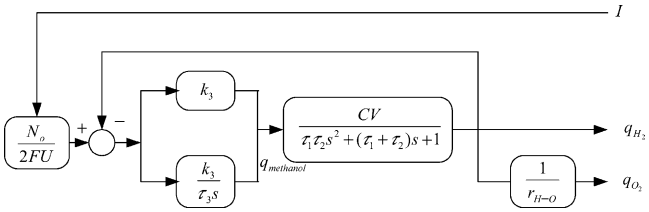

Fig. 2. Reformer and the reformer controller model.

2.2. Reformer model

In Ref. [8], the author introduced a simple model of a reformer that generates hydrogen through reforming methane. The model is a second-order transfer function. The mathematical form of the model can be written as follows:

$$\frac{q_{H_2}}{q_{methane}} = \frac{CV}{\tau_1\tau_2 s^2 + (\tau_1 + \tau_2)s + 1} \quad (1)$$

where $q_{methane}$ is the methane flow rate (kmol/s), CV the conversion factor (kmol hydrogen/kmol methane), τ_1, τ_2 the reformer time constants (s).

To control hydrogen flow according to output power from the fuel cell, a feedback from the stack current is considered. A proportional integral (PI) controller is used to control the flow rate of methane in the reformer [8]. Oxygen flow is determined using the hydrogen–oxygen flow ratio r_{H-O}. The reformer and the reformer controller are illustrated in Fig. 2, where U is the fuel utilization factor, k_3 the PI gain and τ_3 the PI time constant.

2.3. Power conditioning unit model

The power conditioning unit is used to convert dc output voltage to ac. As mentioned before, the power conditioning unit includes a dc/dc converter to raise dc output voltage to dc bus voltage, followed by dc/ac inverter to convert dc bus voltage to ac. In this paper, only a simple model of a dc/ac inverter is considered for the following reasons: the dynamic time constant of inverters is of the order of microseconds or at the most milliseconds. The time constants for the reformer and stack are of the order of seconds. Hence, including the inverter time constant will have negligible effect on the time response accuracy. On the other hand it complicates the system model. All commercial FCPPs have to conform to IEEE standard no. P-1547, which guarantees the ripples in the FCPP's output voltage to be within commercially acceptable limits. A simple model of the inverter is given in Ref. [9]. Considering the fuel cell as a source, the inverter and load connection is shown in Fig. 3. The output voltage and the output power as a function of the modulation index and the phase angle can be written as

$$V_{ac} = mV_{cell}\angle\delta \quad (2)$$

$$P_{ac} = \frac{mV_{cell}V_s}{X}\sin(\delta) \quad (3)$$

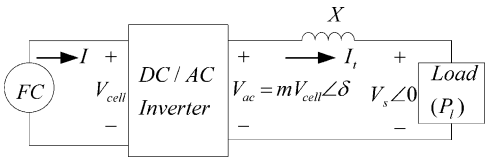

Fig. 3. Fuel cell, inverter and load connection diagram.

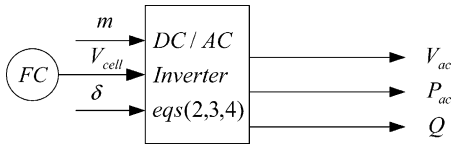

Fig. 4. The dc/ac inverter model.

$$Q = \frac{(mV_{\text{cell}})^2 - mV_{\text{cell}}V_{\text{s}}\cos(\delta)}{X} \tag{4}$$

$$I_{\text{t}} = \frac{P_{\text{l}}}{V_{\text{s}}\cos(\theta)} \tag{5}$$

$$I = mI_{\text{t}}\cos(\theta + \delta) \tag{6}$$

where V_{ac} is the ac output voltage of the inverter (V), m the inverter modulation index, δ the phase angle of the ac voltage mV_{cell} (rad), P_{ac} the ac output power from the inverter (W), Q the reactive power output from the inverter (VAR), V_{s} the load terminal voltage (V), X the reactance of the line connecting the fuel cell to the load (Ω), I_{t} the load current (A), θ the load phase angle (rad) and P_{l} the load power (W) (Fig. 4).

The dc/ac inverter model is shown in Fig. 4. The current feedback signal in Figs. 1 and 2 is calculated from the load information and the ac output voltage. Due to the assumed grid-independent operation the transformer model is not included.

3. Neural network controller

In Ref. [11], the authors introduced a technique to control the active and reactive power output from an FCPP. The proposed technique is based on controlling the inverter modulation index (m) to control the voltage level and the reactive power output from the FCPP. The active power flow from the FCPP to the load is controlled through controlling the phase angle of the ac output voltage (δ). The proposed NN controller uses the same technique proposed in Ref. [11] to control the active and reactive power output from the FCPP. A multilayer feedforward NN with back-propagation training is used. The NN consists of a fully connected three-layer network. The input layer receives four inputs: from the load active power, load reactive power, the ac output voltage magnitude, and the hydrogen input to the FCPP. The hidden layer has 10 neurons with a log-sigmoid activation function. The output layer has two outputs, one to modify the ac voltage phase angle (δ), and the other to modify the modulation index (m). A linear activation function is used for the output layer. The NN configuration is illustrated in Fig. 5.

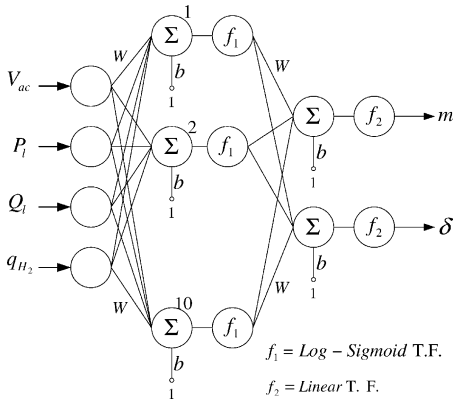

Fig. 5. The proposed NN.

Two sets of data have been used to train the proposed NN. The two sets were produced using the model given in Ref. [11]. The following load profiles were used to produce the training data: (a) computer-simulated step changes in the connected load, (b) actual residential load profiles. The load profiles for a 2500 ft^2 all electric home with two adults and four children were used. The active and reactive power load profiles for a 4 h period (4:48 p.m. to 8:48 p.m.) with a 15 s sampling interval were used.

The training sets were used in a developed software program for training purposes to develop NN structures. The developed NN is in the form of weights and biases to represent the mapping functions between the inputs and outputs. Matlab software is used to train the proposed neural network using the Levenberg–Marquardt technique. The proposed NN and the FCPP block diagram are shown in Fig. 6.

4. Tests and results

The PEM FCPP we currently have in the lab, as well as the commercial FCPPs, need at least an hour to start from cold to build up the reformer and stack temperatures. A minimum load value (critical load) has to be maintained all the time during power plant operation. Decreasing the load below the critical load value will put the FCPP in a sleep or dormant mode, where a small amount of fuel is used to maintain the reformer and stack temperatures at operating levels. Commercially available PEM FCPPs come equipped with storage batteries connected in parallel with the dc bus. These batteries serve as a short-period auxiliary power source to meet load demand that cannot be met by the FCPP, particularly during the transient periods. In the following test cases, the FCPP is assumed to be in the active mode and the initial active and reactive power outputs are 1.0 and 0.0 respectively. Testing the proposed model indicated that the reformer and the reformer controller parameters have significant effect on the power plant time response. The reformer

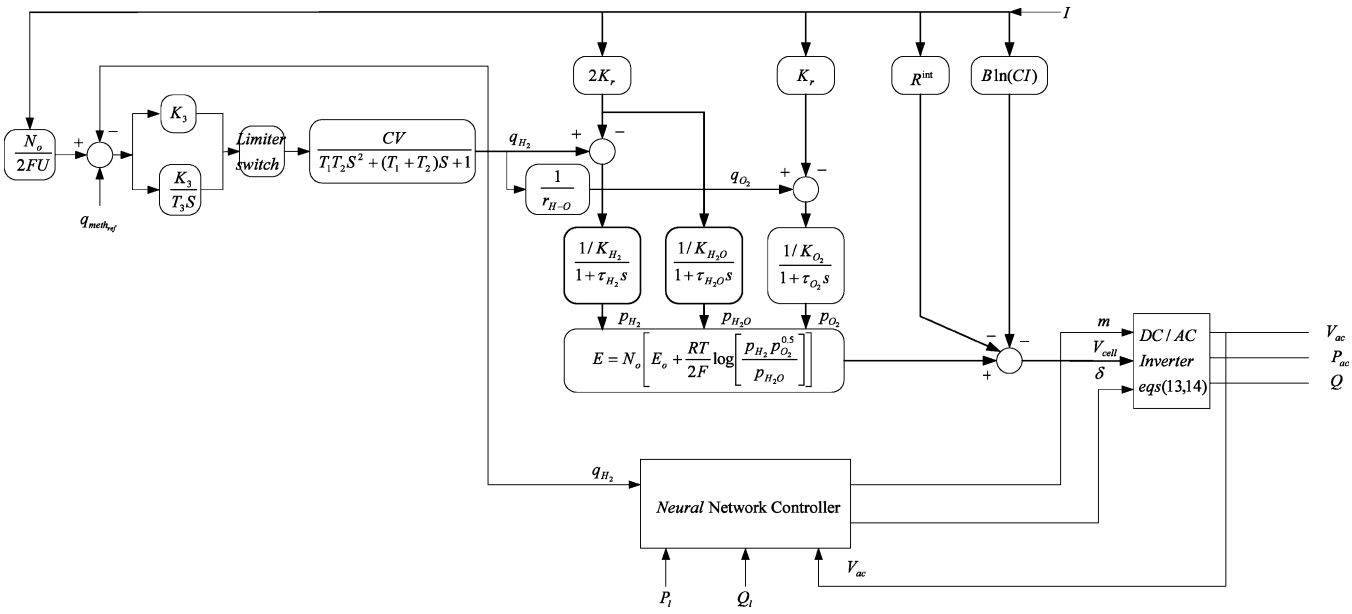

Fig. 6. FCPP system and NN controller block diagram.

parameters affect the reformer damping factor. Choosing a damping factor of 1.0 for the uncontrolled reformer (open loop) is to ensure that no unrealistic overshoot occurs [8]. This will yield $\tau_1 = \tau_2$. For maintaining stability and reasonable fuel processor dynamics of the controlled reformer, the controller parameters are chosen to ensure a damping factor of 0.707 [8]. With this assumption the PI controller time constant τ_3 is equal to τ_1 and k_3 is equal to 1/(2 CV). The model parameters are given in Table 1.

Case 1: The FCPP model shown in Fig. 6 is tested with step changes in the load as shown in Fig. 7. These abrupt changes in the active and reactive power are for testing the dynamic response of the system and do not necessarily represent changes in a residential load. The load model is chosen to reflect all possible variations of active and reactive power. The change of current, voltage, output active and reactive power, output voltage phase angle, modulation index, and flow rate of hydrogen are illustrated in Figs. 8–14. The time interval 0–17 s is not shown in the plots because it represents the dormant state of the FCPP. From these figures, it is evident that an increase in the load increases feedback current, which in turn decreases output voltage of the fuel cell. The increase in current increases methane flow rate and hydrogen flow rate to increase phase angle of output voltage, which increases power flow from the cell to the load. As seen in the ac output power curve, output power has a time delay in following the load power. This is due to the reformer and the fuel cell time constants. Comparison of the results in Ref. [11] and results given in Figs. 8–14 showed

Table 1
Model parameters

Stack temperature, (K)	343
Faraday's constant, F (C/kmol)	96484600
Universal gas constant, R (J/kmol K)	8314.47
No load voltage, E_0 (V)	0.6
Number of cells, N_0	88
K_r constant $= N_0/4F$ (kmol/s A)	0.996×10^{-6}
Utilization factor, U	0.8
Hydrogen valve constant, K_{H_2} (kmol/s atm)	4.22×10^{-5}
Water valve constant, K_{H_2O} (kmol/s atm)	7.716×10^{-6}
Oxygen valve constant, K_{O_2} (kmol/s atm)	2.11×10^{-5}
Hydrogen time constant, τ_{H_2} (s)	3.37
Water time constant, τ_{H_2O} (s)	18.418
Oxygen time constant, τ_{O_2} (s)	6.74
Reformer time constant, τ_1 (s)	2
Reformer time constant, τ_2 (s)	2
Conversion factor, CV	2
Activation voltage constant, B (A^{-1})	0.04777
Activation voltage constant, C (V)	0.0136
Stack internal resistance, R^{int} (Ω)	0.00303
Line reactance, X (Ω)	0.05
PI gain constants, k_5, k_6	10
Voltage reference signal, V_r (p.u.)	1.0
Methane reference signal, $Q_{methref}$ (kmol/s)	0.000015

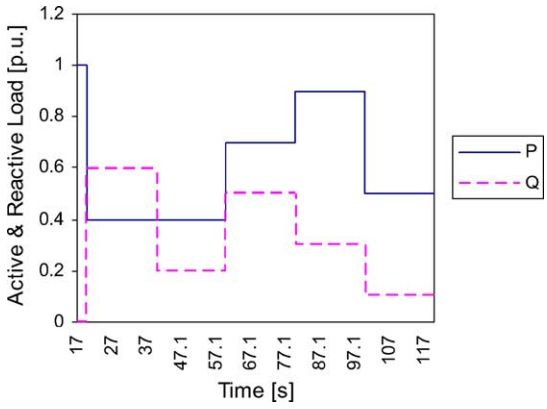

Fig. 7. Load step changes.

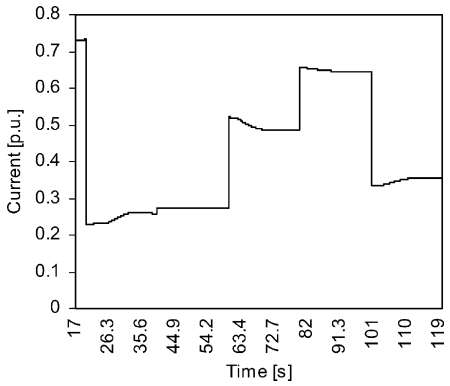

Fig. 8. FC output current.

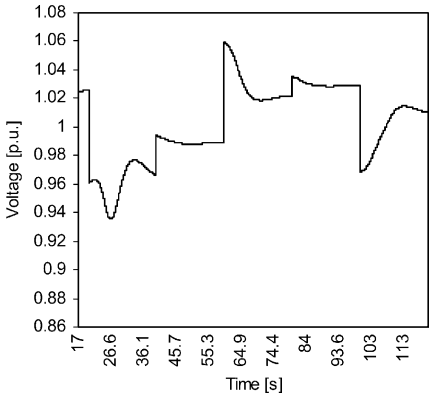

Fig. 9. Ac output voltage.

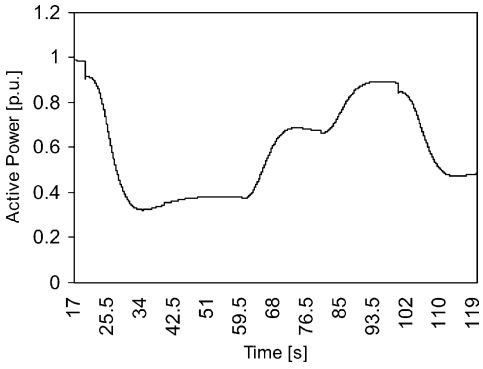

Fig. 10. Active output power.

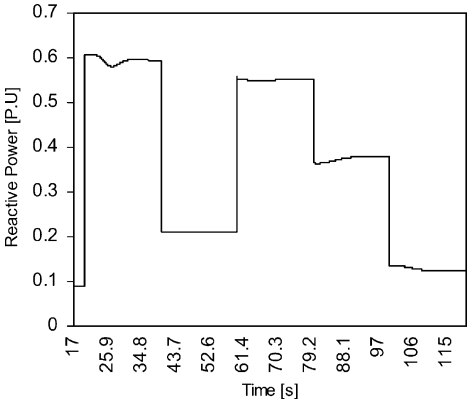

Fig. 11. Output reactive power.

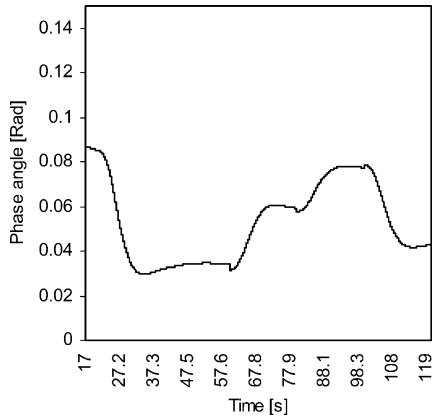

Fig. 12. Output voltage phase angle.

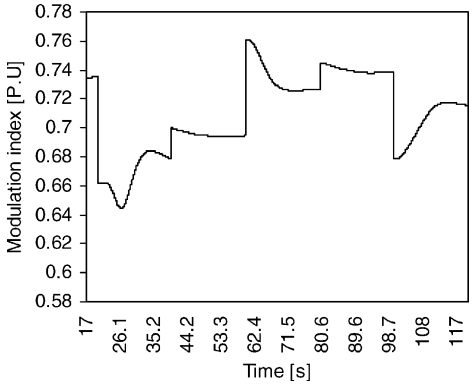

Fig. 13. Modulation index.

that the NN controller was able to modify the phase angle of the ac voltage and the modulation index to conform to the load changes. In addition, the NN controller is characterized by faster time response compared to the PI controllers used in Ref. [11], and this enhances the overall system response.

Case 2: In this test case the model is tested using an actual residential load profile. The load profile for the house mentioned in Section 3 is used. The active and reactive power load profile for a 2 h period (9:00 p.m. to 11:00

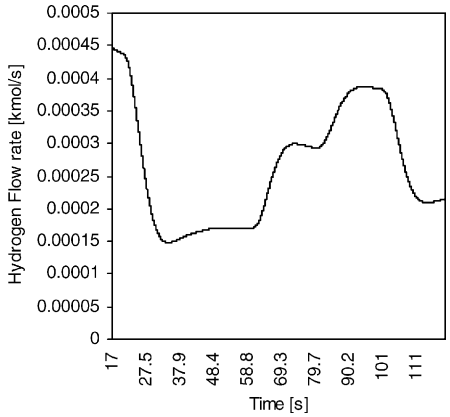

Fig. 14. Hydrogen flow rate.

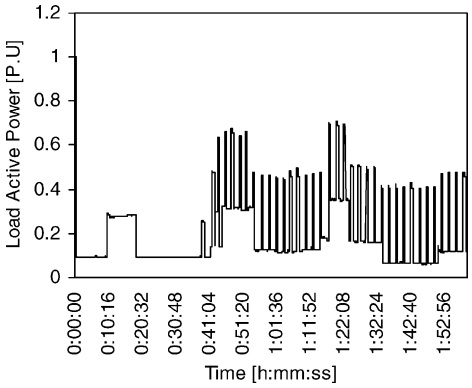

Fig. 15. Residential load active power.

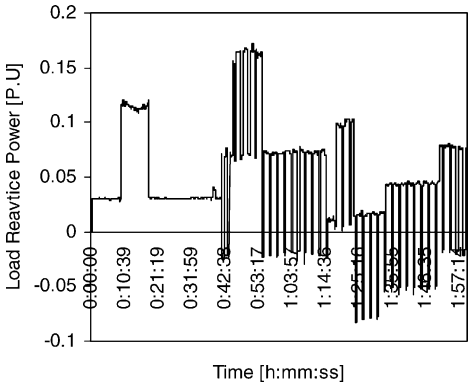

Fig. 16. Residential load reactive power.

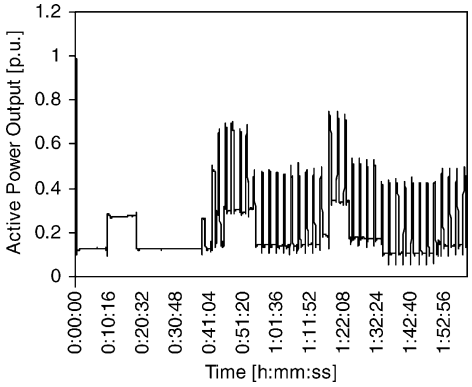

Fig. 17. FC active power output.

p.m.) with a 15 s sampling interval is shown in Figs. 15 and 16. The power and voltage bases are 5 kW and 120 V respectively.

The purpose of this test is to check the load following characteristics of the fuel cell power plant. The active and reactive output powers are shown in Figs. 17 and 18. It can be seen that the FCPP with the embedded NN controller has a fast response to residential load changes and exhibits good load following capability.

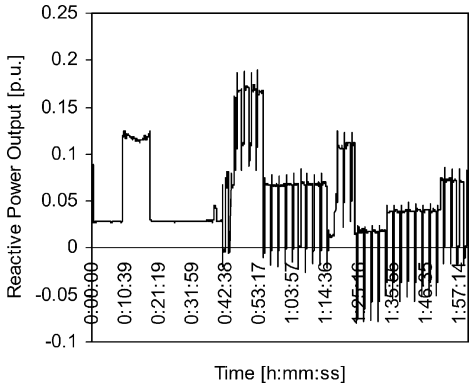

Fig. 18. FC reactive power output.

5. Conclusions

This paper introduces a technique based on neural network to control the active and reactive power output from a stand-alone fuel cell power plant. The paper uses an integrated dynamic model for the fuel cell power plant and a neural network controller to study the time response of the fuel cell. The proposed controller and the fuel cell power plant model have been tested using computer-simulated step changes in the load active and reactive power demands, and actual active and reactive load demands of a single-family residence. The results obtained show rapid response of the controller to load changes, and the effectiveness of the proposed controller for controlling the active and reactive power output. The results also portray the load following capability of the fuel cell power plant.

Acknowledgements

This research was supported by a grant from the Department of Energy (DE-FG02-02ER63376).

References

[1] M.A. Laughton, Fuel cells, Power Eng. J. 16 (1) (2002) 37–47.
[2] S. Um, C.Y. Wang, K.S. Chen, Computational fluid dynamics modeling of proton exchange membrane fuel cell, J. Power Electrochem. Soc. 147 (12) (2000) 4485–4493.
[3] D. Singh, D.M. Lu, N. Djilali, A two-dimension analysis of mass transport in proton exchange membrane fuel cells, Int. J. Eng. Sci. 37 (1999) 431–452.
[4] S. Dutta, S. Shimpalee, J.W. Van Zee, Numerical prediction of mass-exchange between cathode and anode channels in PEM fuel cell, Int. J. Heat Mass Transfer 44 (2001) 2029–2042.
[5] J.C. Amphlett, R.F. Mann, B.A. Peppley, P.R. Roberge, A. Rodrigues, A model predicting transient response of proton exchange membrane fuel cells, J. Power Sources 61 (1996) 183–188.
[6] J. Padulles, G.W. Ault, J.R. McDonald, An integrated SOFC plant dynamic model for power systems simulation, J. Power Sources 86 (2000) 495–500.
[7] M.Y. El-Sharkh, A. Rahman, M.S. Alam, P.C. Byrne, A.A. Sakla, T. Thomas, Proton exchange membrane fuel cell dynamic model for residential use under review, IEEE Trans. Energy Conversion, June 2003.

[8] K. Hauer, Analysis tool for fuel cell vehicle hardware and software (controls) with an application to fuel economy comparisons of alternative system designs, Ph.D. Dissertation, Department of Transportation Technology and Policy, University of California, Davis, 2001.
[9] C.J. Hatziadoniu, A.A. Lobo, F. Pourboghrat, M. Daneshdoost, A simplified dynamic model of grid-connected fuel-cell generators, IEEE Trans. Power Deliv. 17 (2) (2002) 467–473.
[10] J.C. Amphlett, K. Agbossou, A. Laperriere, F. Laurencelle, T.K. Bose, Dynamic behavior of a PEM fuel cell stack for stationary applications, Int. J. Hydrogen Energy 26 (2001) 625–629.
[11] M.Y. El-Sharkh, A. Rahman, M.S. Alam, A.A. Sakla, P.C. Byrne, T. Thomas, Analysis of active and reactive power control of a stand-alone PEM fuel cell power plant, IEEE Trans. Power Systems, in press.